

# A Two-Site Mechanism for ATP Hydrolysis by the Asymmetric Rep Dimer P<sub>2</sub>S As Revealed by Site-Specific Inhibition with ADP–AlF<sub>4</sub><sup>†</sup>

Isaac Wong<sup>‡</sup> and Timothy M. Lohman\*

Department of Biochemistry and Molecular Biophysics, Washington University School of Medicine, 660 South Euclid Avenue, Box 8231, St. Louis, Missouri 63110

Received August 28, 1996; Revised Manuscript Received December 11, 1996<sup>®</sup>

**ABSTRACT:** The *Escherichia coli* Rep helicase is a dimeric motor protein that catalyzes the transient unwinding of duplex DNA to form single-stranded (ss) DNA using energy derived from the binding and hydrolysis of ATP. In an effort to understand this mechanism of energy transduction, we have used pre-steady-state methods to study the kinetics of ATP binding and hydrolysis by an important intermediate in the DNA unwinding reaction—the asymmetric Rep dimer state, P<sub>2</sub>S, where ss DNA [dT(pT)<sub>15</sub>] is bound to only one subunit of the Rep dimer. To differentiate between the two potential ATPase active sites inherent in the dimer, we constructed dimers with one subunit covalently cross-linked to ss DNA and where one or the other of the ATPase sites was selectively complexed to the tightly bound transition state analog ADP–AlF<sub>4</sub>. We found that when ADP–AlF<sub>4</sub> is bound to the Rep subunit in *trans* from the subunit bound to ss DNA, steady-state ATPase activity of 18 s<sup>−1</sup> per dimer (equivalent to wild-type P<sub>2</sub>S) was recovered. However, when the ADP–AlF<sub>4</sub> and ss DNA are both bound to the same subunit (*cis*), then a titratable burst of ATP hydrolysis is observed corresponding to a single turnover of ATP. Rapid chemical quenched-flow techniques were used to resolve the following minimal mechanism for ATP hydrolysis by the unligated Rep subunit of the *cis* dimer: E + ATP ⇌ E–ATP ⇌ E'–ATP ⇌ E'–ADP–P<sub>i</sub> ⇌ E–ADP–P<sub>i</sub> ⇌ E–ADP + P<sub>i</sub> ⇌ E + ADP + P<sub>i</sub>, with  $K_1 = (2.0 \pm 0.85) \times 10^5 \text{ M}^{-1}$ ,  $k_2 = 22 \pm 3.5 \text{ s}^{-1}$ ,  $k_{-2} < 0.12 \text{ s}^{-1}$ ,  $K_3 = 4.0 \pm 0.4$  ( $k_3 > 200 \text{ s}^{-1}$ ),  $k_4 = 1.2 \pm 0.14 \text{ s}^{-1}$ ,  $k_{-4} < 1.2 \text{ s}^{-1}$ ,  $K_5 = 1.0 \pm 0.2 \text{ mM}$ , and  $K_6 = 80 \pm 8 \mu\text{M}$ . A salient feature of this mechanism is the presence of a kinetically trapped long-lived tight nucleotide binding state, E'–ADP–P<sub>i</sub>. In the context of our “subunit switching” model for Rep dimer translocation during processive DNA unwinding [Bjornson, K. B., Wong, I., & Lohman, T. M. (1996) *J. Mol. Biol.* 263, 411–422], this state may serve an energy storage function, allowing the energy from the binding and hydrolysis of ATP to be harnessed and held in reserve for DNA unwinding.

DNA helicases are motor proteins that catalyze transient unwinding of duplex DNA to form the single-stranded (ss) DNA intermediates required for DNA metabolic processes such as replication, recombination, and repair [reviewed in Lohman (1992, 1993), Lohman and Bjornson, (1996), and Matson and Kaiser-Rogers (1990)]. These enzymes capture the chemical bond energy derived from the hydrolysis of nucleoside triphosphates in order to catalyze a change in the conformational state of DNA and therefore share similarities with microtubule and actin-based motor proteins such as kinesin, dynein, and myosin (Hackney, 1994; Gilbert et al., 1995; Schnapp, 1995). However, it is not yet known how this essential process of energy transduction is carried out for any of these motor proteins.

In order to obtain a molecular understanding of the mechanism by which helicases catalyze DNA unwinding and the accompanying energy transduction process, we have been studying the *Escherichia coli* Rep helicase, one of the best

characterized helicases at a mechanistic level [for a recent review see Lohman and Bjornson (1996)]. The *E. coli* rep gene encodes a single polypeptide ( $M_r = 76\,000$ ), and biochemical and genetic studies have established Rep's role in replication of *E. coli* and certain coli phages (Lane & Denhardt, 1975). Although the protein is monomeric in the absence of DNA, it is induced to dimerize upon binding either ss or double-stranded (ds) DNA, and it is this dimeric state that is the functionally active helicase (Chao & Lohman, 1991; Wong et al., 1992; Wong & Lohman, 1992; Amaratunga & Lohman, 1993; Bjornson et al., 1994). Equilibrium binding studies have established that extensive cooperativity exists between the DNA binding sites of the two protomers (subunits) of the dimer, and furthermore, both ss and ds DNA binding affinities are regulated allosterically by nucleotide binding (Wong & Lohman, 1992).

Of central importance to an understanding of energy transduction is elucidation of the elementary mechanism of ATP binding and hydrolysis by the Rep dimer as a function of ss and ds DNA ligation states and the kinetic mechanism of DNA binding as a function of ATP hydrolysis. Toward this end we have used stopped-flow fluorescence techniques to determine the minimal kinetic mechanism for ss DNA binding by Rep and subsequent dimerization in the absence of ATP (Bjornson et al., 1996a). We have also demonstrated that ATP hydrolysis stimulates the rate of a ss DNA exchange

<sup>†</sup> Supported by grants from the National Institutes of Health (GM 45948) and the American Cancer Society (NP-756B). I.W. received partial support from an American Cancer Society postdoctoral fellowship (PF-3671).

\* Address correspondence to this author. Phone: 314-362-4393. FAX: 314-362-4153. E-mail: lohman@biochem.wustl.edu.

<sup>‡</sup> Present address: Department of Biochemistry and Biophysics, Oregon State University, Corvallis, OR 97331.

<sup>®</sup> Abstract published in *Advance ACS Abstracts*, March 1, 1997.

reaction on the Rep dimer (Bjornson et al., 1996b) which has led to important insights into the mechanism of Rep helicase translocation along DNA. Measurements of the steady-state ATPase activities of all three possible Rep–ss DNA complexes,<sup>1</sup> i.e., PS, P<sub>2</sub>S, and P<sub>2</sub>S<sub>2</sub>, have also shown that all three states have dramatically different kinetic properties (Wong et al., 1996). The mechanism of ATP binding and hydrolysis by the Rep monomer has also been solved by transient state methods (Moore & Lohman, 1994a,b).

A major difficulty in obtaining a molecular understanding of the ATPase activity of any multimeric enzyme such as the Rep dimer is that it possesses two potential sites for ATP binding and hydrolysis, one on each subunit, and we have clear evidence for communication between these two sites (Bjornson et al., 1996b). However, neither steady-state ATPase measurements (Wong et al., 1996) nor pre-steady-state measurements on the wild-type P<sub>2</sub>S Rep dimer have enabled us to study the ATPase activities of these two separate sites (K. M. J. Moore, unpublished experiments). Therefore, in this report, we have used alternative approaches to investigate the kinetic mechanism of ATP hydrolysis by the two individual sites of the P<sub>2</sub>S Rep dimer. By using ADP–AlF<sub>4</sub>, a tight binding transition state analog of ATP, in conjunction with Rep protomers covalently cross-linked to ss DNA, Rep–d(T<sub>7</sub>S<sup>2</sup>T<sub>8</sub>) (Wong & Lohman, 1996), we were able to inhibit differentially one or the other of the two ATPase sites of the asymmetric P<sub>2</sub>S Rep dimer. We were thus able to study selectively each of the active sites within the two protomers. We have found that both ATPase sites are active; however, they have dramatically different kinetic properties. Furthermore, this approach has allowed us to solve the mechanism of hydrolysis in the pre steady state for the ATPase site on the protomer not bound to ss DNA. These results have implications in the context of our current model for the mechanism of ATP-driven translocation of the Rep dimer (Bjornson et al., 1996b).

## MATERIALS AND METHODS

**Reagents and Buffers.** [ $\alpha$ -<sup>32</sup>P]ATP (3000 Ci/mmol) was obtained from Amersham, Arlington Heights, IL. Spectrophotometric grade glycerol, HPLC grade methanol, 99% triethylamine, AlF<sub>3</sub>, and 99.99% NaF were obtained from Aldrich (Milwaukee, WI). All solutions were made with reagent grade chemicals, except as noted above, using Milli-Q H<sub>2</sub>O, i.e., distilled H<sub>2</sub>O that was deionized using a Milli-Q water purification system (Millipore Corp., Bedford, MA). All binding experiments and ATPase assays were carried out in BBM buffer: 20 mM Tris-HCl, pH 7.5 at 4 °C, 6 mM NaCl, 5 mM MgCl<sub>2</sub>, and 10% (v/v) glycerol. Triethylammonium bicarbonate buffer (TEAB, 1 M) was made by bubbling CO<sub>2</sub>(g) derived from subliming dry ice into an aqueous solution containing >1 M triethylamine at

0 °C for 4 h or until a pH of 7.5 was achieved; Milli-Q H<sub>2</sub>O was then added to achieve a final concentration of 1 M.

**Proteins, Enzymes, and Oligodeoxynucleotides.** *E. coli* Rep protein was purified to >99% homogeneity from *E. coli* MZ-1/pRepO (Colasanti & Denhardt, 1987) as described (Lohman et al., 1989). Rep concentration was determined spectrophotometrically using  $\epsilon_{280} = 7.68 \times 10^4 \text{ M}^{-1} \text{ cm}^{-1}$  for Rep monomer (Amaratunga & Lohman, 1993). An ATPase-deficient mutant of Rep, K28I, where Lys 28 was replaced with Ile, was constructed and purified to >99% purity as described (I. Wong and T. M. Lohman, manuscript in preparation). Oligodeoxynucleotides were synthesized using an ABI Model PCR-mate 391 DNA synthesizer (Applied Biosystems Inc., Foster City, CA) and purified to >99% homogeneity as described (Lohman & Bujalowski, 1988) and dialyzed (Spectra/Por 7 MWCO 1000) into Milli-Q H<sub>2</sub>O for storage. Oligodeoxynucleotide concentrations were determined spectrophotometrically in 10 mM Tris-HCl, pH 7.5, 1 mM EDTA, and 150 mM NaCl at 25 °C using  $\epsilon_{260} = 1.29 \times 10^5 \text{ M}^{-1} \text{ cm}^{-1}$  per molecule. The oligodeoxynucleotide used for cross-linking to Rep is d(T<sub>7</sub>S<sup>2</sup>T<sub>8</sub>), where S<sup>2</sup> denotes a thymidine derivatized via a linker arm at C5 to a UV reactive nitroarylazido moiety, and the cross-linked Rep–d(T<sub>7</sub>S<sup>2</sup>T<sub>8</sub>) complexes were generated and purified as described (Wong & Lohman, 1996).

**Preparation and Purification of Rep–ADP–AlF<sub>4</sub> Complexes.** Rep–ADP–AlF<sub>4</sub> complexes were prepared by incubating Rep (5.0  $\mu$ M) in BBM buffer containing 20% glycerol, 500  $\mu$ M ADP, 100  $\mu$ M AlF<sub>3</sub> and 500  $\mu$ M NaF at 37 °C for 30 min or at 4 °C for >2 h. The complex was then purified at 4 °C by desalting through a 25 mL Bio-Gel P-60, medium mesh (Bio-Rad, Hercules, CA) column equilibrated in BBM buffer containing 10% glycerol. The complex eluted in the void volume. Purified samples were used within 1 h of preparation or flash frozen in liquid nitrogen and stored at –70 °C. Complexes were stable for >1 week when stored in this manner. At 4 °C, the measured half-life is ~30 h for dissociation of the ADP–AlF<sub>4</sub> (data not shown). Controls performed using radiolabeled ADP–AlF<sub>4</sub> complexes also showed no dissociation of bound ADP during ATP hydrolysis by the other subunit of either Rep dimer (<sup>32</sup>P<sub>X</sub> or PP<sub>X</sub><sup>A</sup>) within the time frame of a typical experiment. Complexes were prepared in this manner for wild-type and DNA cross-linked Rep protein.

**Steady-State ATPase Assay.** ATPase activity was determined at 4 °C by measuring the initial rate of conversion of ATP to ADP using [ $\alpha$ -<sup>32</sup>P] ATP in BBM (20 mM Tris, pH 7.5 at 4 °C, 6 mM NaCl, 5 mM MgCl<sub>2</sub>, 10% glycerol) as described (Wong et al., 1996). Reactions were quenched using 0.5 M EDTA. The extent of ADP formation was monitored by spotting 1  $\mu$ L aliquots at various times onto poly(ethylenimine) (PEI)–cellulose TLC plates (E. Merck, Darmstadt, Germany). TLC plates were developed using 0.3 M potassium phosphate, pH 7.0, as the mobile phase, dried, and imaged on a Betascope 603 direct  $\beta$ -emission imager (Betagen, Waltham, MA). Spots corresponding to radiolabeled ATP and ADP were quantitated using software supplied by the manufacturer.

**Rapid Quenched-Flow ATPase Assay.** For measurement of ATPase activity in the pre steady state, reactions were carried out in a KinTek RQF-3 rapid chemical quenched-flow apparatus (State College, PA) (Johnson, 1986, 1992; Patel et al., 1991) maintained at 4 °C using a circulating

<sup>1</sup> Our nomenclature for Rep–ss DNA species is as follows: P, unligated Rep monomer; PS, Rep monomer bound to single-stranded (ss) DNA (S); P<sub>2</sub>S, Rep dimer with ss DNA bound to one subunit; P<sub>2</sub>S<sub>2</sub>, Rep dimer with ss DNA bound to both subunits; P<sub>2</sub>SD, Rep dimer with one subunit bound to ss DNA and the other subunit bound to double-stranded DNA (D). The nomenclature used for the asymmetric Rep dimer, P<sub>2</sub>S, where one subunit is cross-linked to ss DNA (x) and one subunit is bound to ADP–AlF<sub>4</sub> is as follows: <sup>A</sup>PP<sub>X</sub>, ADP–AlF<sub>4</sub> and the cross-linked ss DNA are on different subunits; PP<sub>X</sub><sup>A</sup>, ADP–AlF<sub>4</sub> and the cross-linked ss DNA are on the same subunit.

refrigerated bath. All reactions were quenched with 0.5 M EDTA, except for the pulse–chase experiments in Figure 5, which were quenched with 1 M HCl. Use of an EDTA quench gave identical results in pre-steady-state experiments as when a cold ATP chase was used. When 1 M HCl was used as the quench, 200  $\mu$ L of  $\text{CHCl}_3$  was immediately added and the solution vortexed in order to denature Rep. The solution was then immediately neutralized with 60  $\mu$ L of 2 M Tris base. In pulse–chase experiments, a solution of nonradiolabeled ATP (200  $\mu$ M final) was used in the quench syringe using a programmed second quench delay time of 0.15 s after which the reaction was quenched with excess EDTA. Reaction products were analyzed by TLC as described above. The effectiveness of EDTA as a quench was verified by the observation that at  $>250$  mM EDTA, the time courses were independent of EDTA concentration.

**Data Analysis.** KINSIM (Barshop et al., 1983) and FITSIM (Zimmerle & Frieden, 1989) were executed on an IBM PS/2 Model 76. NONLIN (Johnson & Frasier, 1985) was executed on a Hewlett-Packard 715. All other data analyses were performed using Kaleidagraph (Synergy Software, Reading, PA) on an Apple Power Macintosh 7100/80AV.

## RESULTS

**Single-Turnover ATPase Experiments.** At Rep concentrations  $>100$  nM (total monomer) and in the presence of 0.5 equiv of  $\text{dT}(\text{pT})_{15}$ , Rep dimerizes to form the asymmetric dimer,  $\text{P}_2\text{S}$ , in which one subunit is bound to  $\text{dT}(\text{pT})_{15}$  while the other subunit remains unligated. Since each monomer of Rep can bind and hydrolyze ATP in the presence and absence of DNA (Moore & Lohman, 1994b; Wong et al., 1996), a dimer contains two potential ATP sites. Furthermore, since the  $\text{P}_2\text{S}$  dimer is asymmetric by virtue of its DNA ligation state, these two sites might be expected to show different kinetic properties. Measurements of the ATPase activity of this ligation state made in the steady state (Moore & Lohman, 1995; Wong et al., 1996), however, failed to show evidence that two active sites were involved in hydrolysis, although on the basis of these steady-state measurements alone, we cannot rule out the possibility of two sites. In order to address this issue directly, we performed ATPase experiments under single-turnover conditions with excess  $\text{P}_2\text{S}$  over ATP as a function of  $\text{P}_2\text{S}$  concentration (Figure 1). At 0.25–1.0  $\mu\text{M}$   $\text{P}_2\text{S}$  and 3 nM ATP, we observed single-exponential kinetics of product formation (Figure 1A). The rates of these reactions were dependent on  $\text{P}_2\text{S}$  concentration in a nearly linear fashion (Figure 1B) indicative of relatively weak binding of ATP with a  $K_{0.5}$  value higher than the accessible range of  $\text{P}_2\text{S}$  concentration. Because of this, we were unable to resolve separate values for  $k_{\text{cat}}$  and  $K_{0.5}$  in a fit to a rectangular hyperbola. However, the ratio,  $k_{\text{cat}}/K_{0.5} = 3.6 \times 10^6 \text{ M}^{-1} \text{ s}^{-1}$ , could be unambiguously obtained from a fit to these data, yielding a lower limit for the apparent second-order rate constant for ATP binding.

The observation in Figure 1 that all of the ATP was hydrolyzed in a single exponential phase rules out the possibility that one ATP molecule could be tightly bound at one site while activating the steady-state ATPase of the other site. Because enzyme is in such large excess over ATP in these experiments, we would not expect binding of two ATP's to the same dimer unless the binding is extremely positively cooperative. However, this was ruled out by the

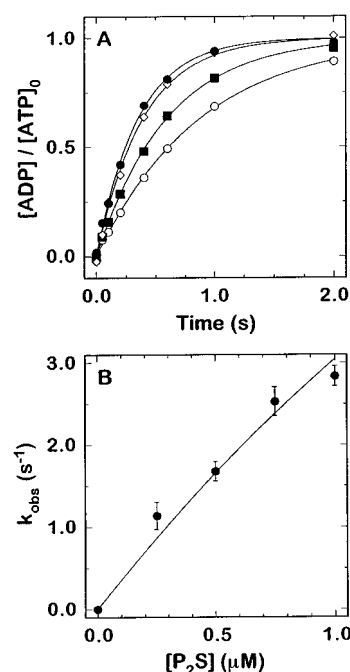


FIGURE 1: Single-turnover ATP hydrolysis by the Rep  $\text{P}_2\text{S}$  dimer.  $\text{P}_2\text{S}$  dimers were formed by premixing Rep monomers with  $\text{dT}(\text{pT})_{15}$  at a molar ratio of 0.5 in BBM buffer at 4 °C. (A) Reactions were carried out at 3 nM  $[\text{ATP}]$  and 0.25 (●), 0.5 (◇), 0.75 (■), and 1.0  $\mu\text{M}$   $\text{P}_2\text{S}$  and quenched with 0.3 M EDTA in a KinTek RQF-3 rapid-quench apparatus. Solid lines represent best fits of the data to single-exponential time courses. (B) The rate constants ( $k_{\text{obs}}$ ) derived from the exponential fits of the time courses in panel A are plotted as a function of  $[\text{P}_2\text{S}]$ . The solid line represents the best fit of the data to a rectangular hyperbola with  $k_{\text{cat}}/K_{0.5} = (3.6 \pm 0.8) \times 10^6 \text{ M}^{-1} \text{ s}^{-1}$ .

fact that the rate of reaction under these conditions was independent of ATP concentration (K. M. J. Moore, unpublished data). Therefore, the two binding sites on the dimer would appear to hydrolyze ATP with very similar kinetic properties or else only one of the two sites is active.

**ADP– $\text{AlF}_4$  Inhibition of Steady-State ATPase.** In order to resolve unambiguously the contributions to ATP turnover from the two potential active sites, we needed to be able to inhibit selectively one of the ATPase sites and examine the ATPase activity of the other active site. We chose to do this with the tight binding inhibitor ADP– $\text{AlF}_4$ , known to be a potent and long-lived inhibitor of a number of ATPases (Fisher et al., 1995; Coleman et al., 1994). When Rep monomers were incubated with  $\text{AlF}_4$  in the presence of ADP and  $\text{MgCl}_2$ , an inhibition complex is formed which is unable to turnover ATP in the presence or absence of  $\text{dT}(\text{pT})_{15}$ . This complex is long-lived with a half-life of reactivation of  $\sim 30$  h at 4 °C and considerably longer when frozen and could be separated from free ADP via gel-filtration column chromatography.

In initial experiments, we mixed Rep–ADP– $\text{AlF}_4$  monomers with wild-type Rep monomers [in the presence of  $\text{dT}(\text{pT})_{15}$  at a 2:1 ratio of total Rep monomers to DNA] and formed statistical mixtures of  $\text{P}_2\text{S}$  in order to examine what effect ADP– $\text{AlF}_4$  bound to one subunit might have on ATP hydrolysis by the other subunit. As shown in Figure 2A, given a 50:50 mixture of inhibited and wild-type subunits, a statistical mixture containing four species of  $\text{P}_2\text{S}$  dimers can be formed assuming that the ss DNA binding and dimerization energetics are the same for each species (this is the case as discussed below). By default, the homodimer

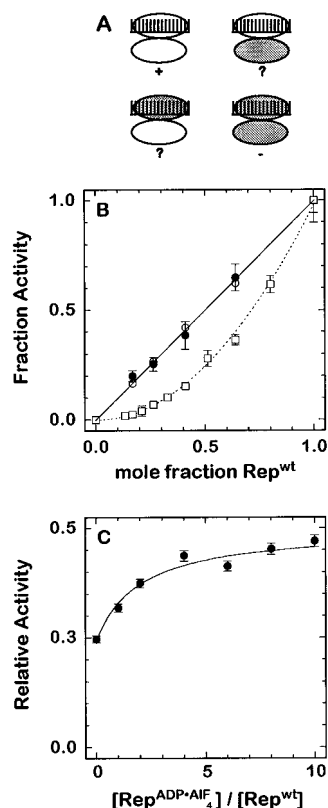


FIGURE 2: Steady-state ATPase activities of Rep P<sub>2</sub>S heterodimers. (A) Cartoon depicting the four possible asymmetric P<sub>2</sub>S dimers formed in a 1:1 molar ratio of active (wild-type) Rep monomers (unfilled) and inactive (either Rep K28I mutant or Rep-ADP-AIF<sub>4</sub>) Rep monomers (shaded). (B) Steady-state ATPase activities were measured at a total concentration of 0.2  $\mu$ M dimers while varying the mole fraction of wild-type subunits vs mutant K28I ( $\square$ ) or Rep-ADP-AIF<sub>4</sub> ( $\bullet$ ) subunits. Control experiments ( $\circ$ ) were carried out with only wild-type subunits without either mutant or ADP-AIF<sub>4</sub> inhibited subunits. The linear behavior of the wild-type + ADP-AIF<sub>4</sub> experiments (described by eq 5b in the Appendix) indicates that only one of the two heterodimers formed with wild-type Rep and Rep-ADP-AIF<sub>4</sub> subunits is active. In contrast, the nonlinear behavior of the wild type + K28I mutant experiments (described by eq 5a in the Appendix) indicates that neither of the heterodimers formed between wild-type Rep and K28I subunits is active. (C) A preformed mixture composed of 0.2  $\mu$ M wild-type Rep subunits, 0.2  $\mu$ M K28I subunits, and 0.2  $\mu$ M dT-(pT)<sub>15</sub> was titrated with increasing concentrations of Rep-ADP-AIF<sub>4</sub> subunits plus equimolar dT-(pT)<sub>15</sub>. The recovery of activity as a function of added Rep-ADP-AIF<sub>4</sub> subunits indicates that the Rep-ADP-AIF<sub>4</sub> subunits are able to form heterodimers with wild-type Rep subunits, with equivalent dimerization energetics. The solid line is well described by eq 4 in the Appendix.

containing two wild-type Rep subunits is fully active, and the homodimer containing two inhibited subunits is fully inactive. The question to be addressed is whether either or both of the heterodimers have ATPase activity.

We examined the steady-state ATPase activity of the mixture of P<sub>2</sub>S species shown schematically in Figure 2A by adding 0.2  $\mu$ M dT-(pT)<sub>15</sub> to a constant total Rep monomer concentration of 0.4  $\mu$ M but varied the molar ratios of ADP-AIF<sub>4</sub>-inhibited monomers to wild-type Rep monomers. As shown in Figure 2B (circles), we observed that the total steady-state ATPase activity increased linearly with the mole fraction of wild-type Rep monomer in the reaction mixture. These results were identical to those obtained in a control experiment where the concentration of wild-type monomers was varied in the absence of any Rep-ADP-AIF<sub>4</sub> subunits.

For comparison, we performed the same mixing experiments using an ATPase defective mutant of Rep, K28I, in place of the ADP-AIF<sub>4</sub>-inhibited complex. In the RepK28I mutant, the conserved lysine at amino acid residue 28 that forms part of the phosphate binding loop has been replaced with isoleucine. The RepK28I mutant has quantitatively the same dT-(pT)<sub>15</sub> binding and dimerization properties as wild-type Rep (I. Wong and T. M. Lohman, in preparation). In stark contrast to the ADP-AIF<sub>4</sub> results, a distinctly nonlinear (second order) dependence of ATPase activity on the wt mole fraction was observed in the K28I mutant experiments such that at a mole fraction of 0.5, only a quarter of the total activity was recovered. These results indicate that only the wild-type homodimer is active and that both wt/K28I heterodimers are inactive. By comparison, the observed linear dependence on the mole fraction observed in the ADP-AIF<sub>4</sub> experiment suggests that one of the two heterodimer species formed with Rep-ADP-AIF<sub>4</sub> subunits retains wild-type steady-state ATPase activity while the other does not.

To rule out the trivial possibility that the ADP-AIF<sub>4</sub>-inhibited complexes were incapable of dimerizing to form P<sub>2</sub>S, we performed a rescue experiment, the results of which are shown in Figure 2C. A mixture of P<sub>2</sub>S complexes was preformed from a 1:1 ratio of wild-type and K28I subunits which had one-fourth of the total wild-type ATPase activity. To this mixture were added ADP-AIF<sub>4</sub> inhibited Rep monomers and an increase in the ATPase activity was observed as a function of added ADP-AIF<sub>4</sub>-Rep monomers. The only way that an increased ATPase activity could result from this experiment is if the ADP-AIF<sub>4</sub>-Rep subunits are capable of dimerizing with the wild-type Rep subunits to form functional dimers. The solid line represents the predicted activity based on a purely statistical model of mixing three species (see Appendix), indicating that the interaction energetics (ss DNA binding and dimerization) among all possible dimer species are comparable.

The results of the RepK28I mutant mixing experiment indicates that both heterodimeric P<sub>2</sub>S species formed between a mutant subunit and a wild-type subunit are inactive in steady-state ATPase. This clearly demonstrates that a communication exists between the subunits across the dimer interface such that activity is obtained only when both subunits are "active". In contrast, the ADP-AIF<sub>4</sub> result suggests that either one of the two heterodimers is active while the other is inactive or else that the wild-type subunits retain full activity, independent of their dimeric state.

**Rep P<sub>2</sub>S Dimers with ADP-AIF<sub>4</sub> and ss DNA Bound to Different Subunits (<sup>A</sup>PP<sub>X</sub>) Are Fully Active in Steady-State ATP Turnover.** To distinguish between these two possibilities and to further probe the molecular aspects of the two ATPase sites, we took advantage of DNA cross-linking technology. We have previously shown that Rep can be covalently cross-linked via an azido group to the ss oligodeoxynucleotide d(T<sub>7</sub>S<sup>2</sup>T<sub>8</sub>) (see Materials and Methods), and the resulting monomer, PX, and singly ligated dimer, P<sub>2</sub>X, complexes both retain the same steady-state ATPase activity as measured for the un-cross-linked complexes, PS and P<sub>2</sub>S (Wong & Lohman, 1996). This enabled us to form Rep dimer complexes in which the ADP-AIF<sub>4</sub> could be specifically targeted to either subunit of the P<sub>2</sub>S dimer. Thus we could form a dimer where the ADP-AIF<sub>4</sub> and the ss DNA are bound to different subunits (a *trans* complex denoted <sup>A</sup>PP<sub>X</sub>) or alternatively form a dimer where the ADP-AIF<sub>4</sub>

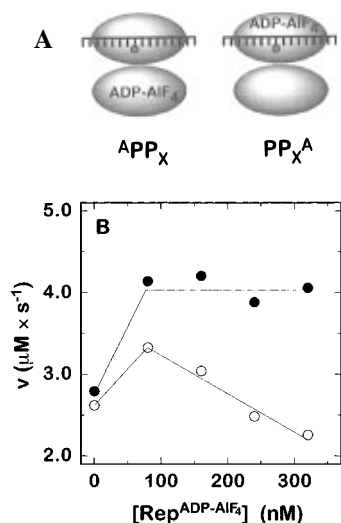


FIGURE 3: Steady-state ATPase activity of Rep  $P_2S$  heterodimers with ADP- $AlF_4$  and ss DNA contained on opposite subunits ( $APP_X$ ). (A) Cartoon depicting the two heterodimers that can be formed by mixing Rep monomers cross-linked to d(T<sub>7</sub>S<sup>2</sup>T<sub>8</sub>) and Rep monomers, either of which had been previously bound with ADP- $AlF_4$ . Nomenclature:  $APP_X$  represents the dimer where ADP- $AlF_4$  is bound in *trans* from the cross-linked ss DNA, while  $PP_X^A$  represents the dimer where ADP- $AlF_4$  is bound to the same subunit that contains the cross-linked ss DNA. (B) The steady-state ATPase activity of the  $APP_X$  dimer was measured by titrating Rep-ADP- $AlF_4$  subunits into a solution of a 0.4  $\mu M$  Rep-d(T<sub>7</sub>S<sup>2</sup>T<sub>8</sub>) mixture (●). Because the Rep-d(T<sub>7</sub>S<sup>2</sup>T<sub>8</sub>) mixture contained only 61% (244 nM) cross-linked subunits, it contained an initial concentration of 0.16  $\mu M$   $P_2S$ , giving rise to a significant initial ATPase activity. However, upon addition of Rep-ADP- $AlF_4$  monomers, the observed ATPase activity increased, indicating that additional  $P_2S$  dimers were formed between the ss DNA cross-linked monomers (PX) and the Rep-ADP- $AlF_4$  monomers and these dimers possess wild-type  $P_2S$  activity. The plateaued value of  $\sim 4 \mu M^{-1} s^{-1}$  corresponds to a  $k_{cat}$  of 20  $s^{-1}$  at 0.2  $\mu M$   $P_2S$ . In a control experiment, Rep-ADP- $AlF_4$  monomers were added to a solution containing 400 nM Rep monomers and 244 nM dT-(pT)<sub>15</sub> (○). Following an initial increase in activity, corresponding to half the magnitude observed with cross-linked subunits, the activity decreased with further addition of Rep-ADP- $AlF_4$  monomers. This decrease in activity is consistent with a redistribution of the dT-(pT)<sub>15</sub> from wild-type Rep subunits to the added Rep-ADP- $AlF_4$  subunits, resulting in  $P_2S$  dimers with no activity since both subunits contain ADP- $AlF_4$ .

is bound to the same subunit as the ss DNA (a *cis* complex denoted  $PP_X^A$ ) (see Figure 3A).

In the first experiment, we tested the ATPase activity of  $APP_X$  by titrating Rep-ADP- $AlF_4$  monomers,  $AP$ , into a solution of cross-linked Rep-d(T<sub>7</sub>S<sup>2</sup>T<sub>8</sub>) monomers, PX. Because the Rep-d(T<sub>7</sub>S<sup>2</sup>T<sub>8</sub>) solution also contained 30% un-cross-linked Rep protomers (Wong & Lohman, 1996), the starting solution had considerable ATPase activity due to the presence of some endogenous  $P_2X$  dimers in addition to PX. However, as Rep-ADP- $AlF_4$  was titrated into this mixture, an increase in ATPase activity was initially observed which then plateaued at a value corresponding to full wild-type  $P_2S$  ATPase of 18  $s^{-1}$  (Figure 3B, filled circles). This indicates that the  $APP_X$  dimer retains the same steady-state ATPase activity as the wild-type  $P_2S$  dimer. In contrast, the control experiment was performed where Rep-ADP- $AlF_4$  was titrated into a solution containing free Rep and dT-(pT)<sub>15</sub> (un-cross-linked). In this case, the activity initially increased but only to half of the extent observed when the DNA was cross-linked. Furthermore, as more Rep-ADP- $AlF_4$  was added, the activity decreased. This was due to the redistri-

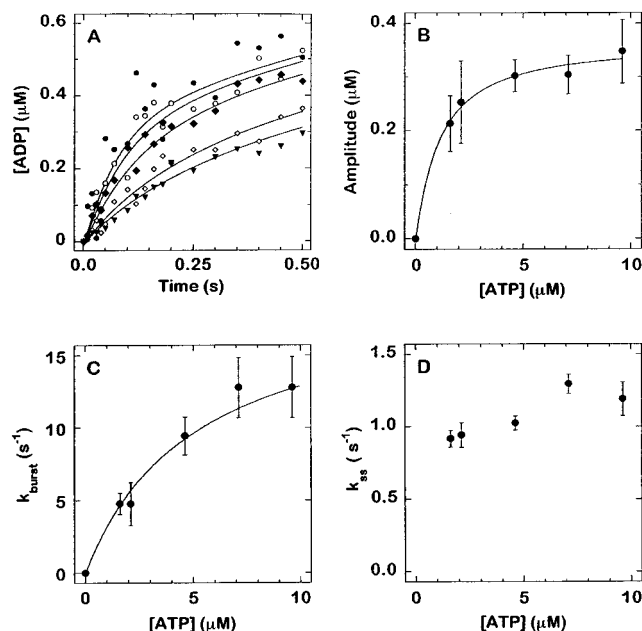


FIGURE 4: Pre-steady-state experiments with  $PP_X^A$  Rep dimers displaying burst kinetics for ATP hydrolysis. (A) The time course of ATP turnover by 0.4  $\mu M$   $PP_X^A$  dimers (see Figure 3A) (BBM buffer, 4 °C) showed biphasic behavior at 9.6 (●), 7.1 (○), 4.6 (◆), 2.1 (◇), and 1.6  $\mu M$  (▼) ATP. (B) The increase in the amplitude of the burst phase with increasing ATP concentration is well described by a rectangular hyperbola with a maximum amplitude of 0.38  $\mu M$  and  $K_{0.5} = 0.5 \mu M$ . (C) The increase in the rate constant of the burst phase ( $k_{obs}$ ) with increasing ATP concentration is well described by a rectangular hyperbola with  $k_{cat} = 22 s^{-1}$  and  $K_{0.5} = 5 \mu M$ . (D) The slow linear phases in the time courses in panel A, yield a steady-state rate constant,  $k_{ss} = 1.2 s^{-1}$ , independent of ATP concentration.

bution of dT-(pT)<sub>15</sub> among all of the  $P_2S$  species, including ones containing two Rep-ADP- $AlF_4$  subunits, which have no activity.

To rule out the trivial possibility that dimerization caused the release of bound ADP- $AlF_4$ , we formed  $APP_X$  dimers using <sup>32</sup>P-labeled ADP and monitored the extent of <sup>32</sup>P remaining bound to Rep during ATP turnover by a nitrocellulose filter binding assay. We observed no dissociation of ADP- $AlF_4$  during ATP turnover (data not shown).

**Rep  $P_2S$  Dimers with ADP- $AlF_4$  and ss DNA Bound to the Same Subunit ( $PP_X^A$ ) Are Active for a Single Turnover.** In a complementary experiment, cross-linked Rep-d(T<sub>7</sub>S<sup>2</sup>T<sub>8</sub>) monomers complexed with ADP- $AlF_4$ ,  $P_X^A$ , were mixed with native wild-type monomers to form  $PP_X^A$  dimers where the DNA and the ADP- $AlF_4$  are bound to the same Rep subunit (see Figure 3A). The intrinsic presence of free Rep in the Rep-d(T<sub>7</sub>S<sup>2</sup>T<sub>8</sub>) preparation (Wong & Lohman, 1996) gave rise to a background amount of Rep-ADP- $AlF_4$  complexes that were not cross-linked to DNA; consequently, it was necessary to add an excess of free Rep in order to form 0.4  $\mu M$   $PP_X^A$  with a final background of 0.4  $\mu M$  free Rep. Since we expected  $PP_X^A$  to have little or no steady-state ATPase activity, we looked directly by rapid quench techniques for a pre-steady-state burst to see if  $PP_X^A$  is competent for a single turnover of ATP hydrolysis.

The time courses of the pre-steady-state experiments are shown in Figure 4A for several ATP concentrations. In each case, we observed a single exponential burst of ADP formation followed by very slow steady-state turnover. The burst amplitude titrated hyperbolically with [ATP] (Figure

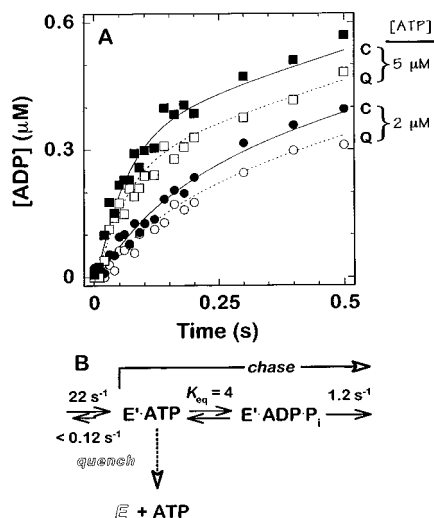


FIGURE 5: Pulse-chase and acid quench experiments monitoring ATP hydrolysis by  $\text{PP}_x^{\text{A}}$  dimers. (A)  $0.4 \mu\text{M}$   $\text{PP}_x^{\text{A}}$  dimers were mixed with  $5 \mu\text{M}$  (■ and □) or  $2 \mu\text{M}$  (● and ○) radiolabeled ATP and either quenched with  $1 \text{ M}$  HCl (□ and ○) or chased with a 100 molar excess of cold ATP (■ and ●), and the time course of ADP formation was monitored by rapid chemical quenched-flow experiments. (B) The results of the pulse-chase experiments indicate that ATP hydrolysis by the  $\text{PP}_x^{\text{A}}$  dimer proceeds via rate-limiting formation of an intermediate state,  $E'$ , at  $22 \text{ s}^{-1}$  in which ATP is tightly bound and in rapid equilibrium with bound (ADP +  $\text{P}_i$ ) with an internal equilibrium constant  $K = 4$  as determined by the excess amount of  $^{32}\text{P}$  ADP released when the reaction is chased with cold ATP vs quenched with acid. The absence of a lag phase in the acid quench reactions indicates that ATP hydrolysis (chemistry step) occurs with a rate constant in excess of  $200 \text{ s}^{-1}$ .

4B), reaching a maximum amplitude of  $0.38 \pm 0.015 \mu\text{M}$  which corresponded well to a single turnover by  $0.4 \mu\text{M}$   $\text{PP}_x^{\text{A}}$ . The rate of the burst phase also titrated hyperbolically with  $[\text{ATP}]$  (Figure 4C), reaching an extrapolated maximum rate of  $22 \pm 3.5 \text{ s}^{-1}$ . However, different  $K_{0.5}$  values of  $0.9 \pm 0.06 \mu\text{M}$  and  $5.0 \pm 1.5 \mu\text{M}$  were measured for the amplitude and the rate, respectively. The slope of the slow linear phase defined the steady-state rate of ATP hydrolysis, with a rate constant  $k_{ss} = 1.2 \pm .14 \text{ s}^{-1}$ , independent of  $[\text{ATP}]$  (Figure 4D).

The observation of burst kinetics followed by a slow steady-state turnover of ATP indicates a rate-limiting step occurring at  $1.2 \text{ s}^{-1}$  after chemical bond cleavage and which is associated with product release. Within the first turnover, however, the rate-limiting step occurs at  $22 \text{ s}^{-1}$ . The hyperbolic dependence of this rate on  $[\text{ATP}]$  indicates that initial binding of ATP occurs in a rapid preequilibrium step. The observed values of  $K_{0.5}$  for the burst amplitude and the burst rate differ because they are sensitive to different elementary steps in the mechanism (see Discussion).

**A Conformational Change Limits the Rate of the First ATP Turnover.** To further investigate the kinetics of the first ATP turnover, we performed a pulse-chase experiment in order to determine if the observed burst rate of  $22 \text{ s}^{-1}$  reflects a true rate of chemical bond cleavage or some rate-limiting conformation change occurring prior to chemistry.  $\text{PP}_x^{\text{A}}$  dimers at  $0.4 \mu\text{M}$  were reacted with ATP ( $10$  or  $2 \mu\text{M}$ ) and either quenched with  $1 \text{ M}$  HCl or chased with a 100-fold excess ( $1 \text{ mM}$  or  $200 \mu\text{M}$ , respectively) of cold ATP, and the results are shown in Figure 5. The HCl-quenched reactions consistently showed a lower extent of product formation as compared to the chased reactions. This

difference is diagnostic of a tightly bound enzyme-ATP complex ( $E' \cdot \text{ATP}$ ) which when chased is capable of partitioning in a net forward flux to yield the additional amount of product observed (see Figure 5B). Furthermore, we did not observe any lag in the HCl-quenched reactions such that the rates of formation of products in both the quenched and chased reactions were identical. This indicates that the formation of this tightly bound enzyme-ATP complex must be the rate-limiting step in the first turnover. Furthermore, the interconversion of enzyme-bound ATP and enzyme-bound  $\text{ADP} \cdot \text{P}_i$  must be rapidly reversible with a net favorable forward equilibrium. The solid lines shown in Figure 5A represent the KINSIM-generated best fits of the data using the model shown in Figure 5B with a rate-limiting conformation change occurring at  $22 \text{ s}^{-1}$  and an internal equilibrium constant of 4 in the forward direction. We estimate that the rate of chemical bond cleavage occurs faster than  $200 \text{ s}^{-1}$  based on the absence of an observable lag in the acid-quenched reaction. The rate of product release was constrained by the steady-state rate to be  $1.2 \text{ s}^{-1}$ . Since a full burst amplitude corresponding to stoichiometric conversion of 1 equiv of bound ATP was observed, the rate of ATP release from the tight complex must be  $< 0.12 \text{ s}^{-1}$  in order to kinetically trap the bound substrate in the tight complex. Otherwise, a lower than stoichiometric burst amplitude would be observed.

**Inhibition of ATPase Activity by ADP and  $\text{P}_i$ .** We next examined the binding of the products, ADP and  $\text{P}_i$ , by measuring their ability to inhibit the rate of ATP hydrolysis in the burst phase. Panels A and B of Figure 6 show the time courses of ATP hydrolysis by  $\text{PP}_x^{\text{A}}$  in the presence of ADP at  $5$  and  $10 \mu\text{M}$  ATP, respectively. The rates of the burst phases are plotted as a function of ADP concentration in Figure 6C. Inhibition was competitive, and the best fit of the data yielded a  $K_i$  for ADP of  $80 \pm 9 \mu\text{M}$ . We also measured the inhibition of the ATPase of  $\text{PP}_x^{\text{A}}$  by inorganic phosphate,  $\text{P}_i$ , the other product of the reaction (Figure 7A), at  $5 \mu\text{M}$  ATP and found that  $\text{P}_i$  also inhibited the reaction competitively with a  $K_i$  of  $1 \pm 0.2 \text{ mM}$  (Figure 7B). Lastly, we performed experiments as a function of ADP concentration in the presence of  $1 \text{ mM}$   $\text{P}_i$  and  $10 \mu\text{M}$  ATP (Figure 8). The nonlinear least-squares fit of the concentration dependence yielded a  $K_i$  for ADP of  $67 \pm 13 \mu\text{M}$ , which is identical, within our uncertainty, to that measured in the absence of  $\text{P}_i$ . These results indicate that binding of ADP and  $\text{P}_i$  is not cooperatively linked and that release of products is not obligatorily ordered, although the vastly weaker binding constant of  $\text{P}_i$  suggests that it is likely released faster than and therefore prior to ADP.

Equilibrium binding constants of this order of magnitude would place the dissociation rate constants for individual products at  $> 1000 \text{ s}^{-1}$ , much faster than the  $1.2 \text{ s}^{-1}$  observed for the step that limits the steady-state rate of turnover. Furthermore, the binding of ADP and  $\text{P}_i$  are not cooperative. Consequently, the  $1.2 \text{ s}^{-1}$  rate-limiting step occurring after chemistry must occur prior to release of either ADP or  $\text{P}_i$  and therefore reflects the rate of relaxation out of the tight binding state after bond cleavage. This assignment is based on several lines of evidence. First, as we have already mentioned, the high  $K_i$  value for  $\text{P}_i$  binding of  $1 \text{ mM}$  suggests that the release of  $\text{P}_i$  likely occurs at rates in excess of  $1000 \text{ s}^{-1}$ . Conversely, assignment of  $1.2 \text{ s}^{-1}$  to  $\text{P}_i$  release would require an association rate constant for  $\text{P}_i$  of  $1.2 \times 10^3 \text{ M}^{-1}$

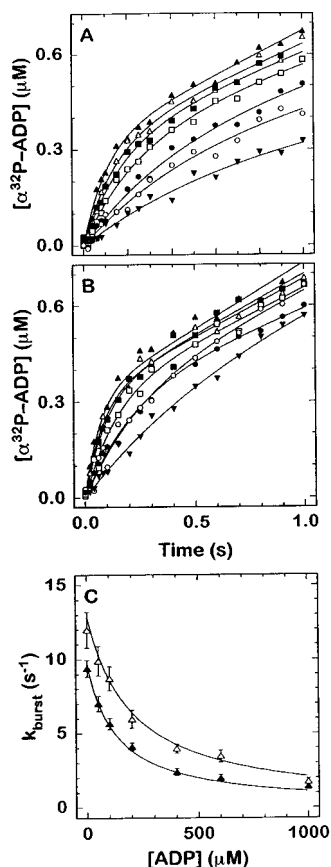


FIGURE 6: Inhibition of the pre-steady-state burst phase by ADP.  $\text{PP}_X^{\text{A}}$  dimers ( $0.4 \mu\text{M}$ ) were reacted with  $5 \mu\text{M}$  ATP (panel A) and  $10 \mu\text{M}$  ATP (panel B) in the presence of 0 ( $\blacktriangle$ ), 50 ( $\triangle$ ), 100 ( $\blacksquare$ ), 200 ( $\square$ ), 400 ( $\bullet$ ), 600 ( $\circ$ ) or 1 mM ( $\blacktriangledown$ ) ADP. (C) The observed rate constants determined for the burst phases are plotted as a function of ADP concentration at 5 ( $\blacktriangle$ ) and 10  $\mu\text{M}$  ( $\triangle$ ) ATP. Solid lines show the best fits of the data to a  $K_i = 80 \mu\text{M}$  for ADP.

$\text{s}^{-1}$ , which is much slower than diffusion control. On the other hand, the pulse-chase experiment clearly indicates a reversible equilibrium between tightly bound substrate and products. Rapid loss of either product would obliterate any such equilibria given the weakness of the binding interactions. We therefore believe that the step with a rate of  $1.2 \text{ s}^{-1}$  represents a relaxation out of the tight complex following hydrolysis just as the  $22 \text{ s}^{-1}$  conformational change step occurring prior to chemistry represents the rate of formation of this tight complex.

## DISCUSSION

The functional forms of all DNA helicases appear to be oligomeric, generally dimeric or hexameric (Lohman, 1992, 1993; Lohman & Bjornson, 1996). One important consequence of these oligomeric structures is that the functional helicase possesses multiple potential sites for ATP binding and/or hydrolysis, as well as multiple potential DNA binding sites. In fact, these multiple ATP sites and DNA sites appear to be essential for DNA helicases to function (Wong & Lohman, 1992; Lohman & Bjornson, 1996; Patel et al., 1994). As such, it is necessary to understand the mode and extent of communication among these sites, which is a challenging experimental problem.

**Two-Site Mechanism of ATP Hydrolysis by the  $P_2S$  Rep Dimer.** The dimeric Rep helicase contains two potential ATP sites, both of which likely play a role in the energy

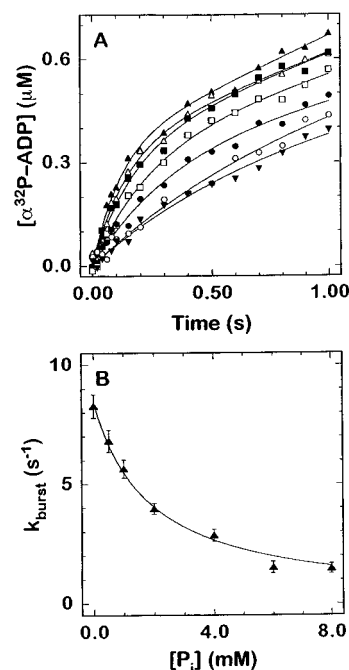


FIGURE 7: Inhibition of the pre-steady-state burst phase by inorganic phosphate,  $\text{P}_i$ . (A)  $\text{PP}_X^{\text{A}}$  dimers ( $0.4 \mu\text{M}$ ) were reacted with  $5 \mu\text{M}$  ATP in the presence of 0 ( $\blacktriangle$ ), 50 ( $\triangle$ ), 100 ( $\blacksquare$ ), 200 ( $\square$ ), 400 ( $\bullet$ ), 600 ( $\circ$ ), and 800  $\mu\text{M}$  ( $\blacktriangledown$ )  $\text{P}_i$ . (B) The observed rate constants for the burst phase are plotted as a function of the  $\text{P}_i$  concentration. Solid lines show the best fit of the data to a  $K_i = 1 \text{ mM}$  for  $\text{P}_i$ .

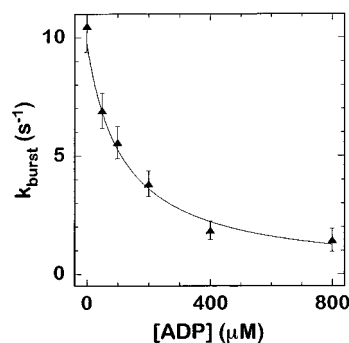


FIGURE 8: Inhibition of the pre-steady-state burst phase by ADP in the presence of inorganic phosphate,  $\text{P}_i$ .  $\text{PP}_X^{\text{A}}$  dimers ( $0.4 \mu\text{M}$ ) were reacted with  $10 \mu\text{M}$  ATP in the presence of 1 mM  $\text{P}_i$  and 0, 50, 100, 200, 400, or 800  $\mu\text{M}$  ADP. The observed rate constants for the burst phase are plotted as a function of ADP concentration, with the solid line representing the best fit of the data to a  $K_i = 66 \mu\text{M}$  for ADP in the presence of 1 mM  $\text{P}_i$ .

transduction process within the functional helicase. In fact, recent studies of the ATP-stimulated dissociation of ss DNA from one subunit of the Rep dimer, which requires transient formation of a  $\text{P}_2\text{S}_2$  intermediate,<sup>1</sup> provide clear evidence for a role for both ATP sites (Bjornson et al., 1996b). In addition, studies of Rep heterodimers containing one wild-type subunit and one mutant (K28I) subunit, such as those shown in Figure 2B, provide direct evidence for the need for communication between the two ATP sites in order for normal hydrolysis to proceed. The asymmetric  $\text{P}_2\text{S}$  Rep dimer, in which one subunit is bound to ss DNA while the other subunit is free of DNA, has been proposed to be an important intermediate in the DNA unwinding reaction (Wong & Lohman, 1992). However, neither steady-state (Wong et al., 1996) nor pre-steady-state studies of ATP hydrolysis by the wild-type  $\text{P}_2\text{S}$  Rep dimer as shown here

Scheme 1

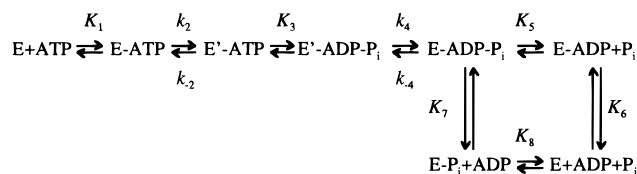


Table 1: Kinetic and Equilibrium Parameters for the ATP Hydrolysis Mechanism

$K_1$	$E + ATP \rightleftharpoons E-ATP$	$(2.0 \pm 0.85) \times 10^5 \text{ M}^{-1}$
$k_2$	$E-ATP \rightleftharpoons E'-ATP$	$22 \pm 3.5 \text{ s}^{-1}$
$k_{-2}$		$< 0.12 \text{ s}^{-1}$
$k_3$	$E'-ATP \rightleftharpoons E'-ADP-P_i$	$> 200 \text{ s}^{-1}$
$K_3$		$4.0 \pm 0.4$
$k_4$	$E'-ADP-P_i \rightleftharpoons E-ADP-P_i$	$1.2 \pm 0.14 \text{ s}^{-1}$
$k_{-4}$		$< 1.2 \text{ s}^{-1}$
$K_5$	$E-ADP-P_i \rightleftharpoons E-ADP + P_i$	$1.0 \pm 0.2 \text{ mM}$
$K_6$	$E-ADP \rightleftharpoons E + ADP$	$80 \pm 8 \text{ } \mu\text{M}$
$K_7$	$E-ADP-P_i \rightleftharpoons E-P_i + ADP$	$1.0 \pm 0.2 \text{ mM}$
$K_8$	$E-P_i \rightleftharpoons E + P_i$	$80 \pm 8 \text{ } \mu\text{M}$

and in other studies (K. J. M. Moore and T. M. Lohman, in preparation) have provided evidence for ATP hydrolysis by both potential ATP sites (Wong et al., 1996).

In the studies reported here, we have successfully dissected the kinetic mechanisms of the two ATPase sites of the asymmetric Rep dimer, P<sub>2</sub>S, by selectively inhibiting one of the ATPase sites using a combination of protein–DNA cross-linking (Wong & Lohman, 1996) and inhibition by complexation with the tight binding transition state analog, ADP–AlF<sub>4</sub> (Fisher et al., 1995; Coleman et al., 1994). We conclude from these studies that both subunits of the P<sub>2</sub>S dimer are kinetically competent but that they show very different kinetics of ATP hydrolysis. The <sup>Δ</sup>PP<sub>X</sub> species (see Figure 3A) does not show burst kinetics in a pre-steady-state experiment and thus the rate-limiting step for hydrolysis occurs before or at chemistry. In fact, the <sup>Δ</sup>PP<sub>X</sub> Rep dimer displays kinetic behavior that is identical to that of wild-type Rep P<sub>2</sub>S dimers. On this basis we conclude that the steady-state ATPase values of  $k_{\text{cat}} = 18 \text{ s}^{-1}$  and  $K_M = 3.1 \text{ } \mu\text{M}$  measured for the wild-type P<sub>2</sub>S dimer (Wong et al., 1996) predominantly reflect ATP hydrolysis by the Rep subunit bound to ss DNA.

However, the ATP site on the subunit not bound to ss DNA is also catalytically active. In fact, pre-steady-state studies show that the PP<sub>X</sub><sup>Δ</sup> Rep dimer (see Figure 3A) displays burst kinetics indicating that it is capable of binding ATP, undergoing a rate-limiting conformational change at  $22 \text{ s}^{-1}$  and hydrolyzing ATP at a rate in excess of  $200 \text{ s}^{-1}$ ; however, the contribution of this subunit to the steady-state rate of ATP hydrolysis is obscured by a rate-limiting step of  $1.2 \text{ s}^{-1}$  occurring after chemistry but before product release. We were further able to determine the elementary steps for catalysis in the non-DNA-containing subunit by pre-steady-state techniques. The resultant minimal kinetic mechanism shown in Scheme 1 with rate and binding constants given in Table 1 quantitatively accounts for all data from the experiments described.

Salient features of this mechanism include rapid preequilibrium binding of substrate, ATP, and products, ADP and P<sub>i</sub>. Following initial binding of ATP, the encounter complex, E–ATP, undergoes a rate-limiting conformational change at  $22 \text{ s}^{-1}$  to form a tight binding intermediate state, E'–ATP,

which is the catalytically active state. Catalysis leading to chemical bond cleavage then proceeds rapidly at a rate in excess of  $200 \text{ s}^{-1}$  with products remaining tightly bound (E'–ADP–P<sub>i</sub>). Substrate and products when bound tightly to Rep in this E' state remain in rapid equilibrium with an internal equilibrium constant,  $K_{\text{int}} = K_3 = 4$ . Relaxation out of this tight state is rate limiting and occurs at  $1.2 \text{ s}^{-1}$  to yield E–ADP–P<sub>i</sub> with subsequent rapid release of products, P<sub>i</sub> and ADP, in a random order. Since we did not observe additional inhibition by the presence of both ADP and P<sub>i</sub> even with extensive preincubation (data not shown), we further conclude that the formation of the tight state, E', from the reverse direction must be unfavorable. Consequently, the rate constant for its formation from the reverse direction ( $k_{-4}$ ) is  $< 1.2 \text{ s}^{-1}$ .

We have previously shown that ATP binding to unligated Rep monomer, P, proceeds by a two-step mechanism under identical solution conditions (Moore & Lohman, 1994a,b). Interestingly, stopped-flow kinetic studies of the binding of both ATP and ATPγS to the P<sub>2</sub>S Rep dimer show a substantial quenching of the intrinsic Rep tryptophan fluorescence accompanying a step occurring after binding of either ATP or ATPγS with a rate constant of  $\sim 22 \text{ s}^{-1}$  (K. M. J. Moore and T. M. Lohman, in preparation). Since quenching is observed for ATPγS as well as ATP, it must reflect a conformational change occurring prior to ATP hydrolysis (i.e.,  $k_2$ ). These stopped-flow studies therefore provide additional independent evidence for a two-step mechanism for ATP binding to the wild-type (uninhibited) P<sub>2</sub>S Rep dimer. Interestingly, the rate constant of  $\sim 22 \text{ s}^{-1}$  for the conformational change observed in the stopped-flow studies is identical to the rate constant we observe for the second step in Scheme 1. It is therefore likely that they both reflect the same global conformational change from E to E'.

The rate constant,  $k_4$ , for relaxation from E' back to E following hydrolysis represents the rate-limiting step during steady-state turnover and a critical step in the reaction pathway with respect to energy transduction and helicase translocation. Unfortunately, attempts to determine the rate constant,  $k_{-4}$ , for the reverse of this step by measuring the overall reverse reaction, i.e., synthesis of ATP from ADP and P<sub>i</sub>, were unsuccessful (data not shown). However, the inability to detect ATP synthesis likely results from the fact that the equilibrium constant,  $K_4$ , for the proposed conformational change E'–ADP–P<sub>i</sub> to E–ADP–P<sub>i</sub> in Scheme 1 is very large, making it difficult to populate E'–ADP–P<sub>i</sub> starting from ADP + P<sub>i</sub>. Further support for this comes from the fact that the product of the remaining equilibrium constants in Scheme 1 ( $K_1 K_2 K_3 K_5 K_6$ ) is significantly smaller than the overall equilibrium constant for ATP hydrolysis of  $\sim 7 \times 10^5 \text{ M}$  (Burbaum & Knowles, 1989) (see Discussion below); thus  $K_4$  must be large and favorable.

An interesting feature of the pre-steady-state kinetic data is that the burst amplitude and the burst rate for the first ATP turnover show different dependencies on ATP concentration (i.e., different values of  $K_{0.5}$ ). While the rate of the first turnover titrated with  $K_{0.5} = 5.0 \text{ } \mu\text{M}$ , the amplitude titrated with a considerably lower  $K_{0.5} = 0.9 \text{ } \mu\text{M}$ . This is consistent with Scheme 1 in that the concentration dependence of the rate of hydrolysis reflects the degree of saturation of substrate binding in the initial rapid equilibrium binding step to form E–ATP and therefore represents an accurate measure of the binding constant for ATP. In



contrast, the burst amplitude reflects the population of kinetically trapped complexes *after* a single-turnover and measures the steady-state concentration of  $E'-ADP-P_i$ . This  $K_{0.5}$ , therefore, reflects the *steady-state*  $K_M$  for ATP hydrolysis for this site.

**ADP-AIF<sub>4</sub> as a Site-Specific Inhibitor.** Our observation of different kinetic behavior for the two ATP sites of the P<sub>2</sub>S Rep dimer hinged on our ability to inhibit selectively each of the two ATP sites in the dimer using a site-specific probe, ADP-AIF<sub>4</sub>. Furthermore, our results explain why we were unable to detect the presence of the two active ATPase sites during steady-state ATP turnover by wild-type P<sub>2</sub>S dimers (Wong et al., 1996). The steady-state ATP turnover rate of 1.2 s<sup>-1</sup> for the subunit not bound to DNA means that, on the average, this site would turnover once for every 16 ATP's hydrolyzed by the subunit bound to ss DNA. Furthermore, because the rate for the first turnover occurs at 22 s<sup>-1</sup>, a value very close to the steady-state rate of 18 s<sup>-1</sup> for the other site, no first-turnover burst of hydrolysis is detectable for the wild-type P<sub>2</sub>S dimer. For this reason, even pre-steady-state experiments did not detect the presence of the two sites (Figure 1 and K. M. J. Moore, unpublished data). We were only able to detect the two sites by knocking out specifically one site and then looking for the remaining activity of the other site.

The use of ADP-AIF<sub>4</sub> as a site-specific inhibitor has both advantages as well as disadvantages. Aside from the obvious advantage already alluded to, ADP-AIF<sub>4</sub> represents a good analog of the transition state during the hydrolysis of ATP. As such, it represents a minimal perturbation of the system. We have shown previously that the Rep dimer displays dramatic global allosteric effects with respect to both nucleotide and DNA binding (Wong et al., 1992, 1996; Wong & Lohman, 1992; Bjornson et al., 1996a,b; Moore & Lohman, 1994a,b). Thus it is a legitimate concern that inhibition of one ATPase site in one subunit of the dimer might perturb the kinetics of ATP turnover in the other. In fact, this is exactly what happens in the Rep heterodimer formed between one wild-type and one mutant (K28I) subunit (Figure 2B and I. Wong and T. M. Lohman, in preparation), which provides evidence for communication between the two ATP sites. On the other hand, for the wt/ADP-AIF<sub>4</sub> heterodimer, the kinetics of hydrolysis of the subunit associated with ss DNA binding are identical to those observed for the native P<sub>2</sub>S dimer in the steady state. This indicates that the ADP-AIF<sub>4</sub> bound at one site does not negatively perturb significantly the ATPase activity at the other site. We believe that the ADP-AIF<sub>4</sub>-bound subunit possesses the characteristics of a subunit that is turning over ATP and thus can promote the global allosteric effects needed to activate the other site. Consequently, its use has provided a unique opportunity to examine one active site of the dimer while the other active site is bound as if it were in the steady state.

The trade-off, of course, comes from our inability to extend our findings to the true first turnover by the dimer when only one site is bound to ATP. Thus we cannot directly address a fundamental question of whether binding and turnover of the very first ATP by one subunit of a dimer activates the ATPase activity of the other subunit. We know from independent studies of the RepK28I mutant (I. Wong and T. M. Lohman, manuscript in preparation) that an essential change in the global conformation of the dimer occurs during or prior to the first turnover, which is required

for achieving steady-state levels of ATP turnover by the P<sub>2</sub>S dimer. However, we are as yet unable to determine which specific ATP binding site is used for this activation process. On the other hand, we note that the single turnover experiments define an apparent second-order rate constant for the first turnover of  $3.6 \times 10^6 \text{ M}^{-1} \text{ s}^{-1}$ , which is within error the same as the  $k_{\text{cat}}/K_M = 4.4 \times 10^6 \text{ M}^{-1} \text{ s}^{-1}$  measured for the PP<sub>x</sub><sup>A</sup> dimer.

**The Role of Two ATP Sites and Implications for Helicase Translocation.** The results of our studies have implications for the mechanism of helicase translocation and DNA unwinding. We have previously postulated that the asymmetric P<sub>2</sub>S Rep dimer is an important intermediate in processive DNA unwinding (Wong & Lohman, 1992) and stepwise translocation along a linear lattice (Bjornson et al., 1996b). In this model, binding of a distal segment of the DNA lattice by the free (with respect to DNA) subunit of the P<sub>2</sub>S dimer leads to transient formation of either a P<sub>2</sub>S<sub>2</sub> or P<sub>2</sub>SD intermediate, depending on whether there is duplex DNA ahead of the helicase. After formation of the P<sub>2</sub>SD complex, duplex DNA is unwound to form a transient P<sub>2</sub>S<sub>2</sub> complex. This is then followed by the release of the ss DNA segment that was initially bound to the first subunit of the dimer, thus resulting in a net exchange of the bound DNA segment and net movement of the dimer along the DNA lattice. This rolling or subunit switching mode of movement is similar to the "hand over hand" mechanism of movement along microtubules proposed for the microtubule motor protein kinesin (Hackney, 1994, 1995; Gilbert et al., 1995).

At an unwinding junction, as shown in Figure 9, the P<sub>2</sub>S dimer can in principle partition into the junction if the "free" subunit binds duplex DNA to form a P<sub>2</sub>SD complex, or alternatively, it can partition away from the junction by binding ss DNA to form a P<sub>2</sub>S<sub>2</sub> complex. During processive unwinding, binding of ds DNA ahead of the fork to form P<sub>2</sub>SD would lead to formation of the productive unwinding complex and the initiation of the next catalytic cycle, whereas binding of ss DNA to form P<sub>2</sub>S<sub>2</sub> would lead to net movement away from the unwinding junction, resulting in the net disruption of processive unwinding. Clearly, efficient unwinding would mandate a preference for the former process which has led us to postulate that DNA unwinding requires formation of a P<sub>2</sub>SD complex (Wong & Lohman, 1992; Amaratunga & Lohman, 1993).

In this context, we note that the intermediate state of P<sub>2</sub>S, E', with tightly bound ATP and ADP-P<sub>i</sub> in rapid equilibrium (step 3 in Scheme 1), may provide an energetic basis for directing the preferential binding of duplex DNA by P<sub>2</sub>S to form the critical unwinding intermediate, P<sub>2</sub>SD. The E' states represent high-energy conformations of the enzyme that are kinetically trapped by the slow rates of relaxation back to E-ATP,  $k_{-2} \ll 0.2 \text{ s}^{-1}$ , and, more importantly, to E-ADP-P<sub>i</sub>,  $k_4 = 1.2 \text{ s}^{-1}$ . The internal equilibrium constant,  $K_3 \approx 4$ , for enzyme-catalyzed ATP hydrolysis to ADP and P<sub>i</sub> is maintained at a value far from the equilibrium constant of  $\sim 7 \times 10^5 \text{ M}$  for hydrolysis of free ATP, as is the case for many ATPases (Burbaum & Knowles, 1989). As a result, most of the energy available from the binding of ATP is kinetically trapped in the E' states. Therefore, we propose that the E' states of the P<sub>2</sub>S Rep dimer are energetically primed for performing the work of DNA unwinding contingent only on the binding of duplex DNA to the second site of the E' state of the P<sub>2</sub>S dimer.

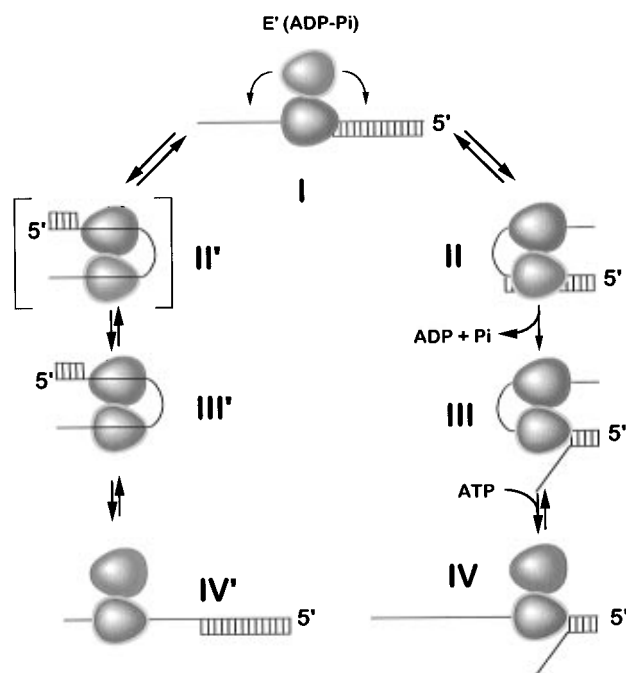


FIGURE 9: Models for energy transduction and the "subunit switching" or "rolling" model of Rep dimer translocation and DNA unwinding. The asymmetric Rep dimer is depicted at an unwinding junction (I). The subunit bound to ss DNA (blue with red outline) is hydrolyzing ATP at a steady-state rate of  $18 \text{ s}^{-1}$ . This constant expenditure of energy maintains the other subunit (red with yellow outline) in its kinetically trapped, tight nucleotide binding conformation,  $E'$  (see Scheme 1). The right side pathway represents binding of duplex DNA to the unligated subunit. Binding of duplex DNA leads to the productive  $P_2S_2$  unwinding complex (II). Unwinding occurs concomitantly with relaxation out of the tight state to yield the transient  $P_2S_2$  state (III). Release of ss DNA from one subunit then regenerates the  $P_2S$  configuration (IV). The left side pathway represents binding of ss DNA to the unligated subunit. Binding of ss DNA by the asymmetric dimer in I leads to formation of the transient  $P_2S_2$  intermediate ( $II'$ ). When this occurs, rapid hydrolysis of ATP ( $70 \text{ s}^{-1}$ ) by the tight binding conformation functions to accelerate release of the ss DNA from one of the subunits ( $III'$ ) in order to regenerate the  $P_2S$  ( $IV'$ ) configuration.

In the event that ss DNA, rather than ds DNA, becomes bound to  $P_2S$ , a competitive  $P_2S_2$  complex will be formed that is nonproductive with respect to DNA unwinding. The top priority if such an event occurs would be to regenerate the  $P_2S$  intermediate as quickly as possible in order to proceed with DNA unwinding. We know that the  $P_2S_2$  complex turns over ATP in the steady state extremely rapidly, at  $>70 \text{ s}^{-1}$  (at  $4^\circ\text{C}$ ), a 4.5-fold increase over the steady-state rate of ATP hydrolysis by  $P_2S$  (Wong et al., 1996). We also have shown that ATP hydrolysis by  $P_2S_2$  enhances the net rate of dissociation of ss DNA from one of the two subunits of the dimer (Wong & Lohman, 1996). Furthermore, by accelerating the release of ss DNA to re-form  $P_2S$  by over 440-fold (at  $4^\circ\text{C}$ ) from  $<0.001 \text{ s}^{-1}$  in the absence of ATP to  $0.44 \text{ s}^{-1}$  during hydrolysis, dimer dissociation ( $0.04 \text{ s}^{-1}$  in the presence of ATP and  $0.007 \text{ s}^{-1}$  in its absence) is circumvented (Bjornson et al., 1996b). Although we do not know the mechanistic details of the switch to this rapidly hydrolyzing mode, its function seems to be quite clear: to regenerate the  $P_2S$  dimer and thus an unligated DNA binding site as quickly as possible.

We emphasize that this high energy state,  $E'$ , is a kinetically trapped state in that relaxation to  $E\text{-ADP-P}_i$  is thermodynamically favorable albeit kinetically slow. Con-

sequently, this state has a finite lifetime and relaxes at a rate of  $1.2 \text{ s}^{-1}$ , when  $\text{ADP-AlF}_4$  is bound in the other subunit. Unfortunately, we do not know the lifetime of this species when no nucleotide or when ATP or ADP is bound in the adjoining subunit. However, an intriguing possibility exists that the lifetime of this species may be increased by the constant expenditure of energy by the Rep subunit bound to ss DNA as it hydrolyzes ATP at  $18 \text{ s}^{-1}$ . In other words, the constant high rate of steady-state ATP hydrolysis by one Rep subunit may function to maintain the dimer in some global conformation that prevents the release of ADP and  $P_i$  from the enzyme active site on the other subunit, thereby trapping the energy required for unwinding in that tight binding conformation,  $E'$ . In this context, the DNA-bound Rep subunit and its constant ATP hydrolysis may serve as the true energy source for the unwinding reaction while the other subunit acts only as a temporary energy storage device much like a capacitor does in an electric circuit.

Lastly, we note that this two ATP site mechanism may also provide an energetic basis for the observed directionality of Rep dimer translocation during processive DNA unwinding without the need to invoke a biased directionality for translocation of the helicase along ss DNA. We have argued previously that net directionality may result from the inherent asymmetry present at the ss/duplex DNA unwinding junction and the observed selective binding of duplex DNA by  $P_2S$  induced by the nonhydrolyzable ATP analog  $\text{AMPP(NH)P}$  (Wong & Lohman, 1992). Our current results provide further evidence for this from the viewpoint of the relationship between ATP hydrolysis and this selectivity. While we cannot rule out the possibility that there may be a structural preference for directional "binding" during translocation, we note that the current model does not require such a structural constraint. We note further that a structural basis for directionality is required for motor proteins such as kinesin, due to the equivalence of all binding sites on the microtubule lattice, whereas for a DNA helicase, the lattice on either side of the helicase is conformationally distinct (ss vs duplex DNA). This important difference may be directly reflected in differences in the mechanism and mode of translocation between these two classes of motor proteins.

## ACKNOWLEDGMENT

These studies benefited greatly from Keith Moore's studies of the wild-type Rep ATPase mechanism. We thank Janid Ali, Keith Bjornson, and Keith Moore for critical discussions and comments on the manuscript and Bill van Zante for synthesis and purification of the oligodeoxynucleotides.

## APPENDIX

In a molar mixing experiment with three components, wild-type subunits, K28I mutant subunits, and  $\text{ADP-AlF}_4$  inhibited subunits, present at concentrations  $A$ ,  $B$ , and  $C$ , respectively, we define  $b$  and  $c$  as the molar ratios of mutant and  $\text{ADP-AlF}_4$  subunits relative to wild-type subunits as defined in eq 1. The probabilities for finding a wild type, a

$$b = \frac{B}{A} \quad c = \frac{C}{A} \quad (1)$$

mutant, and an  $\text{ADP-AlF}_4$  inhibited subunit in the mixture are given by  $\rho_A$ ,  $\rho_B$ , and  $\rho_C$  as defined in eq 2a–c. If the interaction energetics among the three components are

$$\rho_A = \frac{1}{1 + b + c} \quad (2a)$$

$$\rho_B = \frac{b}{1 + b + c} \quad (2b)$$

$$\rho_C = \frac{c}{1 + b + c} \quad (2c)$$

equivalent, then the concentrations of all nine possible dimers are statistically given by the probability of the corresponding pairwise interactions as given in eq 3a–f. Since only the

$$\rho_{AA} = \rho_A^2 = \frac{1}{(1 + b + c)^2} \quad (3a)$$

$$\rho_{BB} = \rho_B^2 = \frac{b^2}{(1 + b + c)^2} \quad (3b)$$

$$\rho_{CC} = \rho_C^2 = \frac{c^2}{(1 + b + c)^2} \quad (3c)$$

$$\rho_{AB} = \rho_{BA} = \rho_A \rho_B = \frac{b}{(1 + b + c)^2} \quad (3d)$$

$$\rho_{AC} = \rho_{CA} = \rho_A \rho_C = \frac{c}{(1 + b + c)^2} \quad (3e)$$

$$\rho_{BC} = \rho_{CB} = \rho_B \rho_C = \frac{bc}{(1 + b + c)^2} \quad (3f)$$

wild-type homodimer and one of the wild-type Rep–ADP–AlF<sub>4</sub> heterodimers are active, the total activity,  $\nu_T$ , is given by the sum of these two probabilities as in eq 4. When only

$$\nu_T = \rho_{AA} + \rho_{AC} = \frac{1 + c}{(1 + b + c)^2} \quad (4)$$

two components are present in an experiment, eq 4 is modified by setting either  $b = 0$  or  $c = 0$  to yield eqs 5a,b.

$$\nu_T = \frac{1}{(1 + b)^2} \quad (5a)$$

$$\nu_T = \frac{1}{1 + c} \quad (5b)$$

Equations 5a and 5b correspond to the case where no Rep–ADP–AlF<sub>4</sub> protomers or mutant protomers are present, respectively. Since the mole fraction of wild-type subunits in a mixture containing wild type and the K28I mutant is given by  $(1 + b)^{-1}$  and the mole fraction of wild-type subunits in a mixture containing wild-type and Rep–ADP–AlF<sub>4</sub> subunits is  $(1 + c)^{-1}$ , eqs 5a,b yield directly the observed squared dependence of activity on the mole fraction of wild type to K28I mutant subunits and the linear dependence of activity on the mole fraction of wild type to Rep–ADP–AlF<sub>4</sub> subunits observed in Figure 2B.

In the experiment where Rep–ADP–AlF<sub>4</sub> subunits and dT(pT)<sub>15</sub> were added to a starting mixture of 1:1 wild-type and mutant subunits, the activity is always measured relative to the fraction of wild-type and mutant subunits, such that even though their absolute concentrations remained constant throughout the experiment, their relative concentrations decrease as more and more Rep–ADP–AlF<sub>4</sub> subunits are added. The resultant relative activity,  $\nu_R$ , is described by eq 6a in general and eq 6b for the case of a 1:1 ratio of wild-type to mutant subunits.

$$\nu_R = \frac{\rho_{AA} + \rho_{AC}}{\rho_A + \rho_B} = \frac{\frac{1 + c}{(1 + b + c)^2}}{\frac{1 + b}{1 + b + c}} = \frac{1 + c}{(1 + b)(1 + b + c)} \quad (6a)$$

$$\text{when } b = 1, \quad \nu_R = \frac{1 + c}{2(2 + c)} \quad (6b)$$

## REFERENCES

- Amaratunga, M., & Lohman, T. M. (1993) *Biochemistry* 32, 6815–6820.
- Barshop, B. A., Wrenn, R. F., & Frieden, C. (1983) *Anal. Biochem.* 130, 134–145.
- Bjornson, K. P., Moore, K. J. M., & Lohman, T. M. (1994) *Biochemistry* 33, 14306–14316.
- Bjornson, K. P., Moore, K. J. M., & Lohman, T. M. (1996a) *Biochemistry* 35, 2268–2282.
- Bjornson, K. P., Wong, I., & Lohman, T. M. (1996b) *J. Mol. Biol.* 263, 411–422.
- Burbaum, J. J., & Knowles, J. R. (1989) *Biochemistry* 28, 9306–9317.
- Chao, K., & Lohman, T. M. (1991) *J. Mol. Biol.* 221, 1165–1181.
- Colasanti, J., & Denhardt, D. T. (1987) *Mol. Gen. Genet.* 209, 382–390.
- Coleman, D. E., Berghuis, A. M., Lee, E., Linder, M. E., Gilman, A. G., & Sprang, S. R. (1994) *Science* 265, 1405–1412.
- Fisher, A. J., Smith, C. A., Thoden, J. B., Smith, R., Sutoh, K., Holden, H. M., & Rayment, I. (1995) *Biochemistry* 34, 8960–8972.
- Gilbert, S. P., & Johnson, K. A. (1994) *Biochemistry* 33, 1951–1960.
- Gilbert, S., Webb, M. R., Brune, M., & Johnson, K. A. (1995) *Nature* 373, 671–676.
- Hackney, D. D. (1994) *Proc. Natl. Acad. Sci. U.S.A.* 91, 6865–6869.
- Hackney, D. D. (1995) *Nature* 377, 448–450.
- Johnson, K. A. (1986) *Methods Enzymol.* 134, 677–702.
- Johnson, K. A. (1992) in *The Enzymes*, pp 1–61, Academic Press, Inc., New York.
- Johnson, M. L., & Frasier, S. G. (1985) *Methods Enzymol.* 117, 301–342.
- Lane, H. E. D., & Denhardt, D. T. (1975) *J. Mol. Biol.* 97, 99–112.
- Lohman, T. M. (1992) *Mol. Microbiol.* 6, 5–14.
- Lohman, T. M. (1993) *J. Biol. Chem.* 268, 2269–2272.
- Lohman, T. M., & Bujalowski, W. (1988) *Biochemistry* 27, 2260–2265.
- Lohman, T. M., & Bjornson, K. P. (1996) *Annu. Rev. Biochem.* 65, 169–214.
- Lohman, T. M., Chao, K., Green, J. M., Sage, S., & Runyon, G. (1989) *J. Biol. Chem.* 264, 10139–10147.
- Matson, S. W., & Kaiser-Rogers, K. A. (1990) *Annu. Rev. Biochem.* 59, 289–329.
- Moore, K. J. M., & Lohman, T. M. (1994a) *Biochemistry* 33, 14565–14578.
- Moore, K. J. M., & Lohman, T. M. (1994b) *Biochemistry* 33, 14550–14564.
- Moore, K. J. M., & Lohman, T. M. (1995) *Biophys. J.* 68, 180s–185s.
- Patel, S. S., Wong, I., & Johnson, K. A. (1991) *Biochemistry* 30, 515–526.
- Patel, S. S., Hingorani, M. M., & Ng, W. M. (1994) *Biochemistry* 33, 7857–7868.
- Schnapp, B. J. (1995) *Nature* 373, 655–656.
- Wong, I., & Lohman, T. M. (1992) *Science* 256, 350–355.
- Wong, I., & Lohman, T. M. (1996) *Proc. Natl. Acad. Sci. U.S.A.* 93, 10051–10056.
- Wong, I., Moore, K. J. M., Bjornson, K. P., Hsieh, J., & Lohman, T. M. (1996) *Biochemistry* 35, 5726–5734.
- Wong, I., Chao, K. L., Bujalowski, W., & Lohman, T. M. (1992) *J. Biol. Chem.* 267, 7596–7610.
- Zimmerle, C. T., & Frieden, C. (1989) *Biochem. J.* 258, 381–387.